frontiers in Materials

ORIGINAL RESEARCH
published: 02 March 2022
doi: 10.3389/fmats.2022.775333

Enhanced Thermal and Antibacterial Properties of Stereo-Complexed Polylactide Fibers Doped With Nano-Silver

*Shiyou Zhao[1†], Huizhen Ke[2†], Tingting Yang[1], Qiqi Peng[1], Jianlong Ge[1], Lirong Yao[1], Sijun Xu[1], Ding Zhirong[1] and Gangwei Pan[1]**

[1]National and Local Joint Engineering Research Center of Technical Fiber Composites for Safety and Protection, School of Textile and Clothing, Nantong University, Nantong, China, [2]Fujian Key Laboratory of Novel Functional Textile Fibers and Materials, Minjiang University, Fuzhou, China

Stereo-complexed polylactide (sc-PLA) fibers with excellent heat resistance and antibacterial properties were prepared by electrospinning. Due to poor heat resistance, common poly(L-lactide) (PLLA) fibers have poor dimensional stability at high temperatures and cannot be sterilized and recycled as a medical filter material. In this research, PLLA/poly(D-lactide) (PDLA) blends doped with silver nanoparticles (AgNPs) were electrospun to obtain the sc-PLA fibers. The effect of thermal induction temperature on the crystalline structure and thermal properties of sc-PLA fibers was investigated. Moreover, the influence of the addition amount of AgNPs on the crystal structure of sc-PLA fibers was studied, and the antibacterial properties of the sc-PLA fibers with different addition amounts of AgNPs were analyzed. The thermal induction is beneficial to the formation of stereo-complexed crystals of sc-PLA fibers, and finally completely stereo-complexed PLA fibers were obtained. The melting temperature of the completely stereo-complexed PLA fibers was 50°C higher than that of the PLLA fibers; therefore, the sc-PLA fibers have better heat resistance. The addition of AgNPs was conducive to the formation of stereo-complexed crystals of sc-PLA fibers. In addition, the antibacterial rate of sc-PLA fibers against *E. coli* and *S. aureus* was 99.99 ± 0.01% when the addition amount of AgNPs was only 0.15 wt%. The fiber membrane obtained in this experiment can be used as a reusable filter material, and the sc-PLA fiber membrane has broad application prospects in the biomedical field.

Keywords: stereo-complexed polylactide, AgNPs, heat resistance, crystal structure, antibacterial properties

OPEN ACCESS

Edited by:
Bomou Ma,
Donghua University, China

Reviewed by:
Ratiram Gomaji Chaudhary,
Seth Kesarimal Porwal College, India
Jian Xing,
Anhui Polytechnic University, China

****Correspondence:***
Gangwei Pan
pangangwei@ntu.edu.cn

[†]These authors have contributed equally to this work

Specialty section:
This article was submitted to Polymeric and Composite Materials, a section of the journal Frontiers in Materials

Received: *13 September 2021*
Accepted: *09 February 2022*
Published: *02 March 2022*

Citation:
Zhao S, Ke H, Yang T, Peng Q, Ge J, Yao L, Xu S, Zhirong D and Pan G (2022) Enhanced Thermal and Antibacterial Properties of Stereo-Complexed Polylactide Fibers Doped With Nano-Silver. Front. Mater. 9:775333. doi: 10.3389/fmats.2022.775333

INTRODUCTION

Polylactide (PLA) is a kind of thermoplastic aliphatic polyester with high strength and high modulus (Amani et al., 2019; Kang et al., 2019; Hamad et al., 2020; Sanusi et al., 2020). Because of its origin from renewable resources (such as corn, starch) and biodegradability, it has attracted more attention (Zhang et al., 2015; Boonluksiri et al., 2020). In recent years, research interest in developing durable PLA materials used in automobiles, electronics, and other fields has increased (Pan et al., 2017). In addition, PLA has become one of the most popular polymers for the new generation of biomedical products due to its biocompatibility. PLA is widely used in the biomedical field and food packaging

and medical materials, which require antibacterial properties to ensure safety for PLA products (Lv et al., 2018). However, the thermal and mechanical properties of PLA are not excellent (Yang et al., 2020), and the production and consumption of PLA used for plastic bags, straws, textiles, and other products are still negligible, comparing to petroleum-derived counterparts.

Stereo-complexation between poly(L-lactide) (PLLA) and poly(D-lactide) (PDLA) can improve the thermal and mechanical properties of PLA. PLA with stereo-complexation is named as stereo-complexed polylactide (sc-PLA). The thermal and mechanical properties of sc-PLA are superior to those of PLLA and PDLA (Arias et al., 2015; Phattarateera and Pattamaprom, 2020; Su et al., 2020), so sc-PLA is more stable than PLLA and PDLA (Narita et al., 2013; Zhao et al., 2019). Until now, sc-PLA fiber is usually prepared by melt spinning (Baimark et al., 2019) or solution spinning (Srisuwan and Baimark, 2018), but these spinning methods require high temperature (Boonluksiri et al., 2020) or high-stretching to obtain consistent stereo-complexed crystallites (sc-crystallites).

Electrospinning is a special fiber manufacturing process. The polymer solution or melt is spun in a strong electric field. Electrospinning could produce fibers with a very high specific surface area and porous structure (Chaudhary et al., 2019; Mishra et al., 2019; Septiyanti et al., 2020; Septiyanti et al., 2020). The effect of the applied electric field and the rapid solidification of polymers leads to the extension of macromolecular chains, thereby promoting the formation of sc-crystallites (Monticelli et al., 2014; Brzezinski and Biela, 2015; Spinella et al., 2015). Similar to previous research studies on mechanical stretching of PLLA/PDLA blend fibers during spinning or heat treatment, the extension of the macromolecular chains resulting from electrostatic force will increase interaction between the PLLA and PDLA segments, which will lead to formation and growth of sc-crystallites.

The electrospun fiber could adjust fiber diameter, crystallinity, and molecular chain orientation (Maleki et al., 2015; Maleki et al., 2017), which is very suitable for biomedical applications. The antibacterial properties of materials are very important for biomedical applications (Boonluksiri et al., 2020). Adding antibacterial substances is an effective way to enhance the antibacterial properties of PLA materials. Inorganic antibacterial agents have good safety, thermal stability, and durability. Among inorganic antibacterial agents, silver ion is the most widely used antibacterial agent. Compared with cadmium, copper, lead, and other metal ions, silver ion has strong antibacterial activity and low toxicity.

Silver nanoparticles (AgNPs) can be used as broad-spectrum antimicrobial agents for Gram-positive and Gram-negative bacteria in biomedical and food packaging applications (Potbhare et al., 2020a; Potbhare et al., 2020b; Saravanakumar et al., 2021). Because of high reactivity resulting from the large surface area to volume ratio, AgNPs can efficiently eliminate bacteria and yeasts even at relatively low concentrations (Satoungar et al., 2016). In addition, when the bacteria die, AgNPs will be released and combined with other bacteria again to carry out repeated sterilization.

Recent studies have shown that biomedical materials prepared with PLA/AgNPs have good biocompatibility and antibacterial properties (Li et al., 2021). Moreover, because of good biodegradability of PLA, PLA materials containing AgNPs have a larger application value in textiles and biomedical fields (Ma and Tang, 2017). sc-PLA has higher thermal stability and mechanical properties than PLA. If AgNPs can improve the antibacterial properties of sc-PLA, even at high temperatures, sc-PLA products such as medical materials and food packaging will perform well. However, there are still few studies on sc-PLA/AgNPs.

In this research, sc-PLA fibers and sc-PLA/AgNPs composite fibers were prepared by electrospinning, and PDLA and PLLA fibers were also prepared as control. The effect of the thermal induction and the addition of AgNPs on the crystal structure and properties were investigated. Therefore, the PLLA/PDLA (1:1) blend was used as the raw material to prepare electrospun fiber membranes, and the morphology of the electrospun fiber was observed using a scanning electron microscope (SEM). Differential scanning calorimetry (DSC) was used to study their thermal properties. The Fourier transform infrared spectroscopy (FTIR) test and X-ray diffractometer (XRD) were performed on the sample to characterize its crystal structure, and the antibacterial activity was studied to evaluate sc-PLA fibers and sc-PLA/AgNPs composite materials used in food packaging and medical applications.

EXPERIMENTAL SECTION

Materials

The PLLA (6202D, the weight average molecular weight is 1.6×10^5) used in this study was from NatureWorks in the United States, and the PDLA (the weight average molecular weight is 1.8×10^5) was synthesized in the laboratory. The molecular weight of PLLA and PDLA is measured by gel permeation chromatography (GPC). Analytically pure trichloromethane was purchased from Shanghai Lingfeng Chemical Reagent Co., Ltd., China, and used as a solvent for preparing polymer solutions. The concentration of nano-silver is 4,000 ppm, and the size of AgNPs is about 20 nm, which is prepared in the laboratory. *E. coli* (ATCC25922) and *S. aureus* (CMCC(B)26003) were purchased from Shanghai Luwei Technology Co., Ltd., China, and nutrient broth and phosphate buffered saline (PBS, 0.03 mol/L, pH 7.2) were purchased from China Best Biotechnology Co., Ltd., and nutrition Agar was purchased from Shanghai Bo Microbiology Technology Co., Ltd., China. The chemicals are used without further purification.

Preparation of Spinning Solution

The PLLA and PDLA pellets were dissolved in chloroform with a polymer concentration of 200 g L^{-1}, which were dissolved for 24 h. The PLLA/PDLA spinning solution was the equal mixture for PLLA spinning solution and PDLA spinning solution. In order to prepare fibers with antibacterial properties, 0.15wt%,

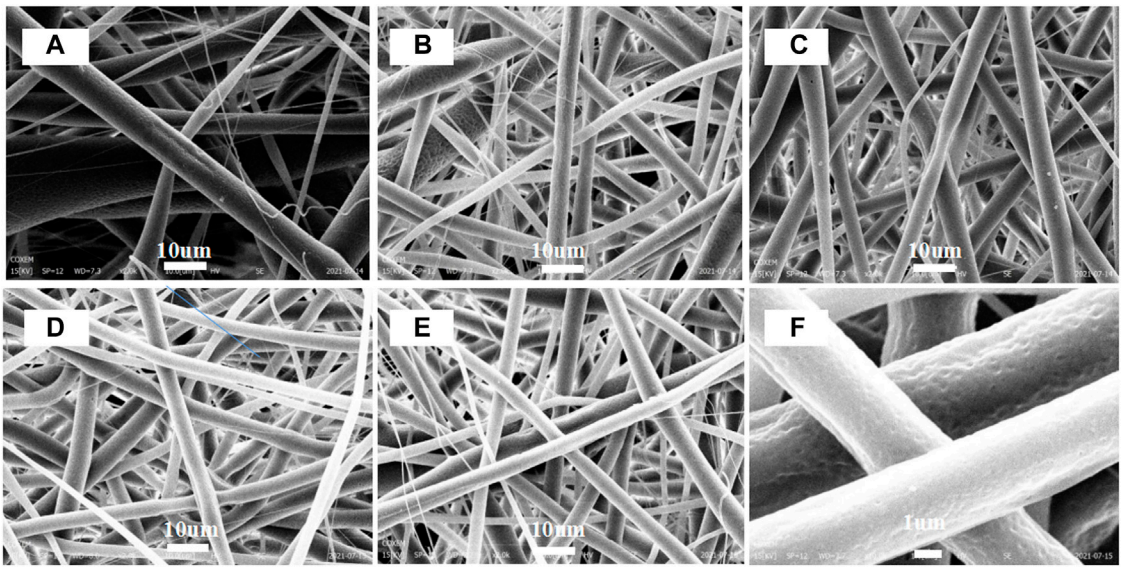

FIGURE 1 | SEM of electrospun fibers: **(A)** PDLA, **(B)** PLLA, **(C)** sc-PLA, **(D)** sc-PLA 120°C, **(E)** sc-PLA 120°C–200°C, and **(F)** high magnification sc-PLA 120°C–200°C.

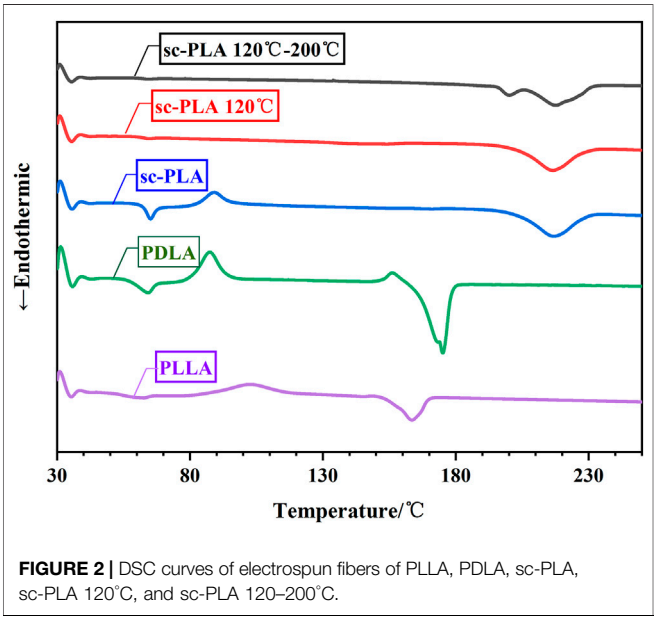

FIGURE 2 | DSC curves of electrospun fibers of PLLA, PDLA, sc-PLA, sc-PLA 120°C, and sc-PLA 120–200°C.

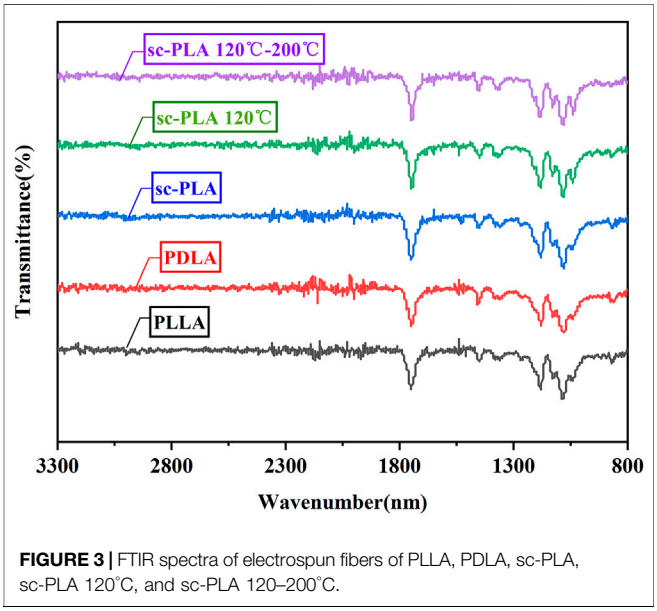

FIGURE 3 | FTIR spectra of electrospun fibers of PLLA, PDLA, sc-PLA, sc-PLA 120°C, and sc-PLA 120–200°C.

TABLE 1 | Thermal performance characteristics of electrospun fibers of PLLA, PDLA, sc-PLA, sc-PLA 120°C, and sc-PLA 120–200°C.

Fiber	T_g (°C)	T_{cc} (°C)	ΔH_{cc} (J/g)	T_m (°C)	ΔH_m. (J/g)
PLLA	61.7	102.4	26.4	167.1	29.1
PDLA	64.4	87.4	37.8	175.1	76.8
sc-PLA	65.2	89.1	21.3	216.9	53.4
sc-PLA 120°C	-	-	-	216.7	52.8
sc-PLA 120–200°C	-	-	-	217.7	52.9

0.30wt%, 0.45wt%, and 0.60wt% AgNPs were added to the mixed PLLA/PDLA solution.

Electrospinning

The electrospun fibers were prepared using electrospinning equipment (HZ-11 Electrospinning Machine, Qingdao Nuokang Environmental Technology Co., Ltd., China). The spinning is conducted at the spinning voltage of 15 kV and the syringe advancing speed of 2 ml/h. The distance between

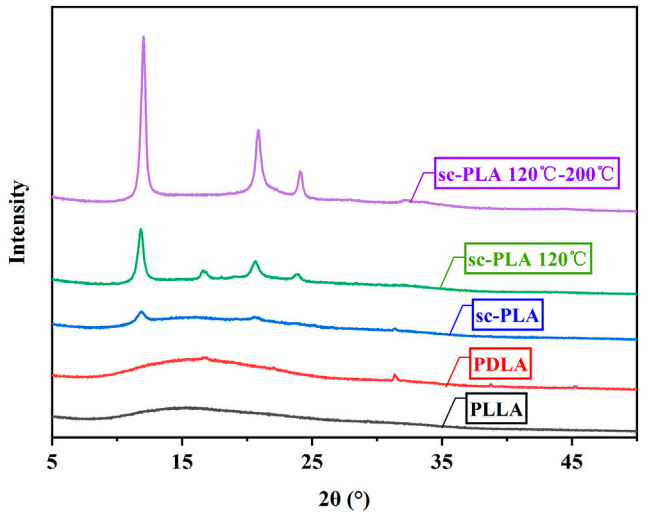

FIGURE 4 | XRD patterns of electrospun fibers of PLLA, PDLA, sc-PLA, sc-PLA 120°C, and sc-PLA 120–200°C.

the needle tip and the fiber collection device is 13 cm, and the winding speed is 200 r/min (Xu et al., 2019; Cao et al., 2020). The electrospun fiber of aforementioned spinning solution under same process conditions was named as PLLA, PDLA, sc-PLA, sc-PLA + 0.15 wt%AgNPs, sc-PLA + 0.30 wt%AgNPs, sc-PLA + 0.45 wt%AgNPs, and sc-PLA + 0.60 wt%AgNPs electrospun fiber membranes. The sc-PLA fiber membranes with AgNPs were all treated in an oven at 120°C for 1 h to obtain sc-PLA 120°C fiber membranes, and then sc-PLA 120°C fiber membranes were treated in an oven at 200°C for 30 min to obtain sc-PLA 120°C–200°C fiber membranes.

Characterization

Scanning Electron Microscope

The EM-30 (COXEM Company, South Korea) scanning electron microscope was used to observe the surface morphology of fibers at an accelerating voltage of 15 kV. Before SEM observation, spraying a layer of gold on the surface of the sample was carried out. All samples before spraying gold were dried in the open air at room temperature for about 5 days and then were measured and observed.

Differential Scanning Calorimetry

Thermal analysis of the electrospun fiber membrane was conducted using an NETZSCH 214 Polyma differential scanning calorimeter under a nitrogen atmosphere. The fibers were heated from 30°C to 250°C at a heating rate of 10°C/min.

X-Ray Diffraction Measurement

The crystal structure of fibers was measured using a Rigaku X-ray diffractometer (Ultima IV, Tokyo) with a Cu-K_α source. The diffractograms of the fibers were performed at 40 kV and 40 mA with scanning angles of 5–50 at a scanning rate of 3°min^{-1}. The X-ray diffraction patterns were analyzed using Jade 5.0 software.

Fourier Transform Infrared Spectroscopy

Fourier transform infrared spectroscopy was carried out on a Nicolet iS10 spectrometer (Thermo Fisher Nicolet, USA) in the wavenumber range of 600–4,000 cm^{-1} using 32 scans. Attenuated total reflection (ATR) method accessory in transmission mode was used to record.

Antibacterial Properties

Antibacterial experiments were performed on *E. coli* (ATCC 25922) and *S. aureus* (CMCC (B) 26003). In short, 0.0375 g sample was added into a centrifuge tube containing 3.75 ml of bacterial suspension, then fixed the centrifuge tube on a shaker at 24°C and 150 rpm for 18 h, and then used 100 μL of the extracted bacterial suspension with 900 μL of bacterial suspension. Phosphate buffer saline (PBS) with pH = 7.2–7.4 was serially diluted $\times10^1$, $\times10^2$, $\times10^3$, and $\times10^4$ and then added dropwise to the agar plate to count the colonies after 24 h of constant temperature culture. No sample group was considered as a control and calculated the antibacterial activity according to the following formula:

$$Y = \frac{W_t - Q_t}{W_t} \times 100\%.$$

In the formula, Y is the bacteriostatic rate of the sample (%), W_t is the viable concentration of the control sample in the flask after 18 h of shaking contact (cuf/mL), and Q_t is the viable concentration of the antibacterial sample in the flask after 18 h of shaking and contact concentration of bacteria (cuf/mL).

RESULTS AND DISCUSSION

The Effect of Thermal Induction on PLLA/PDLA Fibers

Morphology

First, PLLA, PDLA, and sc-PLA were electrospun under the same process conditions to obtain their respective fiber membranes, and then the obtained sc-PLA fiber membranes were treated at a high temperature of 120°C for 1 h. The obtained sc-PLA fiber membrane after 120°C (named sc-PLA 120°C) was treated at 200°C for 30 min to obtain sc-PLA 120–200°C. The morphology of the aforementioned samples is shown in **Figure 1**.

Figure 1 shows that the regularity of fiber fineness is large. As shown in **Figures 1A–C**, The diameter of the coarse fiber and the fine fiber is obviously different, and the number of coarse fiber is more than the number of fine fiber. This may be due to the high concentration of PLLA/PDLA solution (Tsuji et al., 2010; Liu et al., 2011; Liu et al., 2020). The formation of coarse fibers is due to the increase of solution viscosity at high concentrations and molecular aggregation during the electrospinning process. The spinning trickle is difficult to be stretched (Maleki and Barani, 2020). Based on the surface of the fiber (**Figure 1F**) under high magnification SEM, it can be found that there are densely small holes on the surface of the fiber. This is due to the use of chloroform as the solvent, which evaporated rapidly during

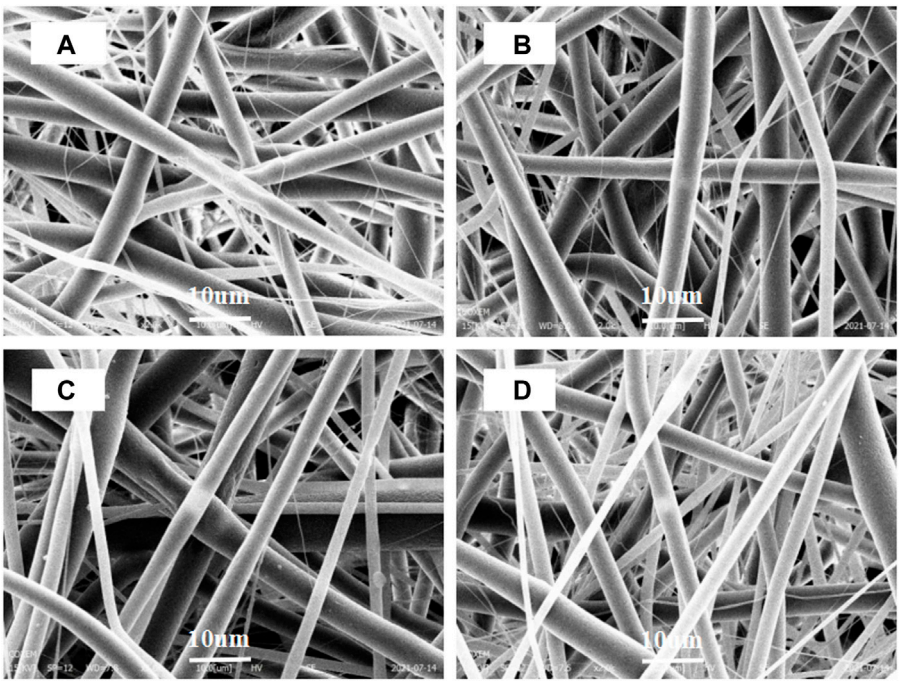

FIGURE 5 | SEM of sc-PLA electrospun membranes with AgNPs: **(A)** sc-PLA + 0.15 wt%AgNPs **(B)** sc-PLA + 0.30 wt%AgNPs, **(C)** sc-PLA + 0.45 wt%AgNPs, and **(D)** sc-PLA + 0.60 wt%AgNPs.

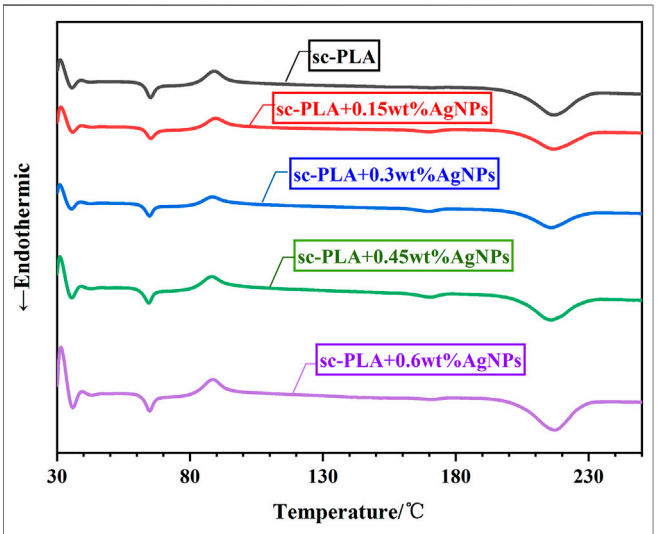

FIGURE 6 | DSC curves of sc-PLA electrospun membranes with different AgNP contents.

the spinning process. **Figure 1** also demonstrates that thermal induction has slight effect on the morphology of the electrospun fibers of sc-PLA at 120°C (**Figure 1D**) and sc-PLA at 120°C–200°C (**Figure 1E**). Since crystals have already existed in sc-PLA fibers before thermal induction, the crystals are prone to maintain the shape of the fibers during thermal induction (Pan et al., 2018).

Thermal Properties

Figure 2 shows the DSC thermograms of electrospun fibers of PDLA, PLLA, sc-PLA, sc-PLA 120°C, and sc-PLA 120–200°C. **Table 1** summarizes the thermal properties of electrospun fibers obtained from DSC analysis. It can be seen from **Figure 2** that sc-PLA only has an endothermic peak in the temperature range of 210–220°C, comparing to PDLA (170–180°C) and PLLA (160–170°C). This was mainly ascribed to the sc-crystallites. The melting temperature of the homo-crystallites in PLLA or PDLA is around 170°C, while the melting of the sc-crystallites in the sc-PLA is nearly 220°C. It can also be seen that the sc-PLA fiber spun using the electrospinning process has a high degree of sc-crystallites. Because the stretching and orientation of the macromolecular chains caused by high voltage during the electrospinning process can enhance the orientation of the macromolecular chains and promote the formation of sc-crystallites. Additionally, a drawing force induced by the electric field could increase the specific surface area of the molecular chain and enhance the interaction between the PLLA and PDLA chains, resulting in rapid crystallization of sc-crystallites (Yamamoto et al., 2015).

Figure 2 also shows that sc-PLA fibers have glass transition temperature of 55°C and cold crystallization temperature of 85°C. However, there are no corresponding endothermic and exothermic peaks at 55°C and 85°C for sc-PLA 120°C and sc-PLA 120–200°C. After thermal induction treatment at 120°C and 200°C, the molecular chain segments in the crystalline region have been perfected, and the mobility of the molecular chain segments in the amorphous region is greatly reduced; therefore, the melting endothermic peak of sc-crystallites appears only in the temperature range of 210–220°C.

TABLE 2 | Crystal sizes of different polymers.

sc-PLA		sc-PLA 120°C		sc-PLA 120–200°C	
Peak position	**Crystal size (nm)**	**Peak position**	**Crystal size (nm)**	**Peak position**	**Crystal size (nm)**
11.9°	12.46	11.9°	16.17	11.9°	19.68
20.7°	11.21	20.7°	13.66	20.7°	16.93
-	-	23.9°	15.61	23.9°	21.78

TABLE 3 | Thermal properties of electrospun fibers of sc-PLA, sc-PLA + 0.15 wt% AgNPs, sc-PLA + 0.30 wt% AgNPs, sc-PLA + 0.45 wt% AgNPs, and sc-PLA + 0.60 wt% AgNPs.

Fiber	T_g (°C)	T_{cc} (°C)	T_m (°C)	ΔH_m (J/g)
sc-PLA	65.2	89.1	216.9	53.4
sc-PLA + 0.15 wt% AgNPs	65.3	89.6	216.5	40.67
sc-PLA + 0.30 wt% AgNPs	64.8	88.5	215.9	34.92
sc-PLA + 0.45 wt% AgNPs	64.5	88.1	215.8	51.07
sc-PLA + 0.60 wt% AgNPs	64.8	88.7	217.0	65.76

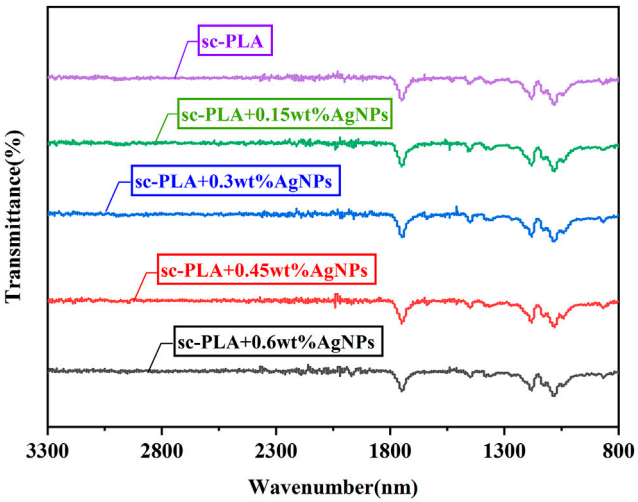

FIGURE 7 | FTIR curves of sc-PLA electrospun membranes with different AgNP contents.

There is a small endothermic peak at around 200°C for the sc-PLA 120°C–200°C, which is a double peak. This is due to incomplete crystallization of sc-crystallites (Sawai et al., 2007; Saeidlou et al., 2012).

FTIR Spectra

Figure 3 shows the FTIR diagrams of different polymers. Compared with PDLA and PLLA fibers, sc-PLA fibers have strong intermolecular forces. As shown in **Figure 3**, the bands associated with methyl groups in sc-PLA fibers shift from 2,941 to 2,939 cm^{-1}. The frequency shift of the methyl group (CH_3-) is attributed to the hydrogen bonding between the PLLA and PDLA molecules in the sc-PLA fiber (Pan et al., 2018). It shows that during heat treatment, the molecular chain segments have been rearranged.

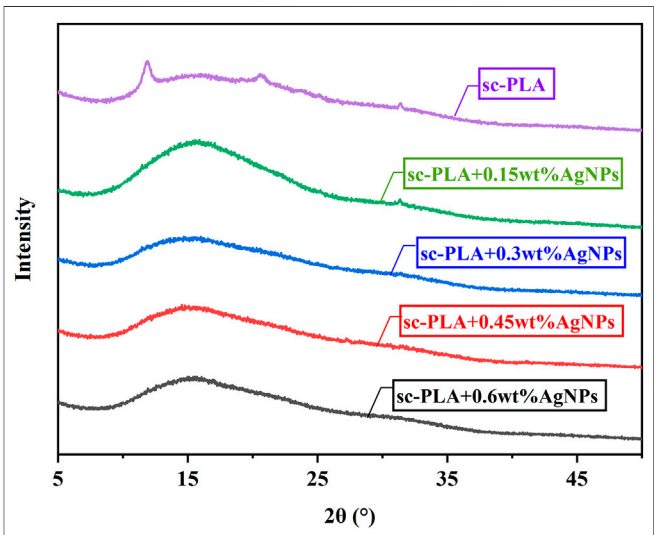

FIGURE 8 | XRD curves of sc-PLA electrospun membranes with different AgNP contents.

Crystal Structure

The same conclusion can be drawn in the XRD diagram (**Figure 4**). The electrospun fiber membrane before thermal induction shows only a small diffraction peak at 16°, indicating that the fiber membrane before thermal induction has low degree of homo-crystallites. As shown in **Table 2**, the diffraction pattern of thermally induced fibers shows obvious diffraction peaks at 11.9°, 20.7°, and 23.9°, which corresponds to the characteristic diffraction peaks of sc-crystallites. It shows that more sc-crystallites are formed after thermal induction, as the molecular chains of sc-PLA are stacked in parallel in a triclinic unit cell in a 3_1-helix structure. (Furuhashi et al., 2006).

THE EFFECT OF AGNPS ON PLLA/PDLA FIBERS

Morphology

It can be seen from **Figure 5**, the fibers of sc-PLA + 0.15 wt% AgNPs, sc-PLA + 0.30 wt% AgNPs, sc-PLA + 0.45 wt% AgNPs, and sc-PLA + 0.60 wt% AgNPs are prepared by adding AgNPs, and no micron-sized AgNPs were found on the surface of electrospun fibers. This indicates that submicron AgNPs can be uniformly dispersed in the sc-

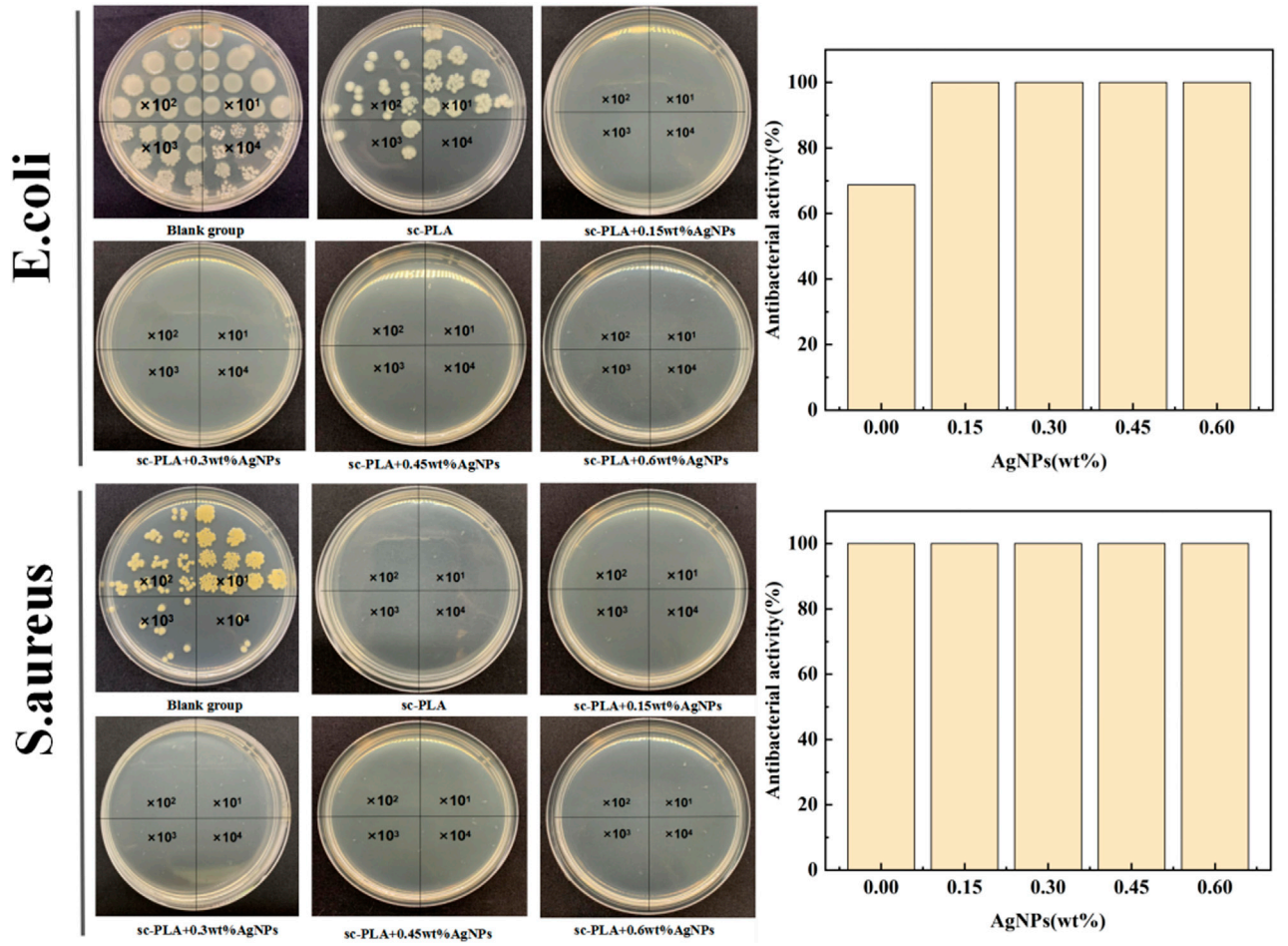

FIGURE 9 | Antibacterial activity of sc-PLA electrospun membranes containing AgNPs against *E. coli* and *S. aureus*.

PLA matrix, but the addition of AgNPs does not significantly change the spinnability of the sc-PLA solution.

Thermal Properties

Figure 6 shows the DSC curves of sc-PLA with different AgNP contents, and the relevant data resulting from the DSC curves are listed in **Table 3**. As shown in **Figure 6** and **Table 3**, there is a relatively insignificant peak around 170°C. In addition, the fusion enthalpy of sc-PLA fiber was lower than that of sc-PLA + 0.60 wt % AgNPs fiber but was higher than that of other three fibers. It indicates that the addition of AgNPs can affect the formation of sc-crystallites and homo-crystallites to a certain extent. Moreover, research on the influence of the addition of AgNPs on the formation of sc-crystallites will be conducted in subsequent research.

FTIR Spectra

Figure 7 shows the FTIR curves of electrospun sc-PLA fiber membranes with different AgNP contents. Similar to sc-PLA electrospun fiber membranes, the bands at 2,992 cm^{-1} and 1743 cm^{-1} are related to methyl and carbonyl groups in the fiber, respectively. The addition of AgNPs has no effect on the position of each group in the molecular chain of sc-PLA, so the electrospun fiber membranes containing AgNPs do not change the chemical structure of sc-PLA.

Crystal Structure

From the XRD curves of fibers with different AgNP contents in **Figure 8**, it can be seen that there are some slight sc-crystallites diffraction peaks for sc-PLA fiber membranes, but there is no obvious crystal diffraction peak for fiber membranes with AgNPs. This is ascribed to poor crystallinity of electrospun fibers. The reason is that in the electrospinning process, even though the crystallization ability of sc-crystallites is stronger than that of the homo-crystallites and the jet is highly stretched and the solvent volatilizes quickly, the molecular chain still does not have enough time to adjust the conformation to form a regular stacking of crystals. It can be seen that before thermal induction, even with the addition of AgNPs, it does not significantly improve the crystallization ability of the sc-PLA fiber membranes. The

synergistic effect of the addition of AgNPs and the thermal induction process on crystallization need be investigated further.

Antibacterial Properties Analysis

PLA is the degradable material with antibacterial and antifungal properties because PLA materials will form an acidic environment during use, which is not conducive to bacterial growth. Compared with the blank control group, the untreated sc-PLA fiber membranes have antibacterial properties against *S. aureus* and *E. coli*. As shown in **Figure 9**, the antibacterial effect of the sc-PLA fiber membranes against *S. aureus* is better than against *E. coli*. The inhibition rate for *E. coli* is 68.75 ± 2.54%, while the inhibition rate for *S. aureus* reaches 99.99 ± 0.01%, which may be due to the different cell wall composition and structure of the bacterial strains (Jing et al., 2019). AgNPs impart stronger antibacterial effect on the sc-PLA fiber. When the addition amount of AgNPs is 0.15 wt%, the antibacterial rate against *E. coli* and *S. aureus* both reaches 99.99 ± 0.01%.

This is because the cell membrane of bacteria is generally negatively charged; once it comes into contact with positively charged metal ions, it will be tightly adsorbed under the action of Coulomb force, and at the same time, silver ions can enter the cell and react with the sulfhydryl group (-SH) on the protein, which makes the protein denatured and inactivated, and the cell loses the ability of reproduction and metabolism. At the same time, the antibacterial rate also depends on the resistance of the bacteria's structure to the reactive oxygen species (ROS) generated on the surface of nanomaterials. The nature of active oxygen is due to the large surface area and small particle size of nanoparticles that increase oxygen vacancies. As the oxygen vacancies increase, more types of reactive oxygen species will eventually lead to cell death. Silver ions can activate oxygen in the air or water to produce hydroxyl free radicals (OH^-) and reactive oxygen ions. Finally, these free radicals collide with electrons to inhibit or kill bacteria (Potbhare et al., 2019). Similarly, when the addition amount of AgNPs increased to 0.30 wt%, 0.45 wt%, and 0.60 wt%, the inhibitory rates against *E. coli* and *S. aureus* are all 99.99 ± 0.01%.

CONCLUSION

In this research, electrospinning was used to prepare sc-PLA fibers from a mixing solution of PLLA and PDLA at a ratio of 1: 1. The structure and properties of the fibers before and after thermal induction treatment and adding AgNPs were characterized. The SEM image clearly showed that the electrospun fiber was relatively coarse, and the thermal induction had no obvious influence on the fiber diameter. It was obvious that the AgNPs existed in the electrospun fiber in the form of submicron. In addition, the melting temperature of sc-PLA fiber increased by 40–50°C, compared to that of PLLA or PDLA. After thermal induction, the molecular chain segments of the fiber could be rearranged to some extent, and the thermal induction is more conducive to the formation of sc-crystallites, so the degree of sc-crystallites of sc-PLA fiber increased. The addition of AgNPs had a slight effect on the formation of sc-crystallites of sc-PLA without thermal induction but had significant effect on the antibacterial properties. In addition, the electrospun sc-PLA fiber had excellent antibacterial effect against *Staphylococcus aureus*. After adding AgNPs, the antibacterial rate against both *Escherichia coli* and *Staphylococcus aureus* reached 99.99 ± 0.01%. Moreover, the synergetic effect of addition amount of AgNPs and thermal induction on the structure and properties of sc-PLA fiber will be investigated subsequently.

DATA AVAILABILITY STATEMENT

The original contributions presented in the study are included in the article/Supplementary Material, further inquiries can be directed to the corresponding author.

AUTHOR CONTRIBUTIONS

SZ and HK: data curation, investigation, and writing—original draft. TY, QP, and LY: methodology. GP: supervision. JG, DZ, and SX: review and editing. All authors contributed to the article and approved the submitted version.

FUNDING

The authors are grateful to the Inner Mongolia Science and Technology Plan (zdzx2018060), National Key Research and Development Program of China (2021YFC2600301), Postgraduate Research Practice Innovation Program of Jiangsu Province (SJCX21_1451), Natural Science Foundation of Jiangsu Province (BK20190925), Jiangsu Advanced Textiles Engineering Technology Center Program (XJFZ/2021/6), Jiangsu Key Research and Development Program (BE2021025), and Nantong Municipal Science and Technology Program (MS12020050 and MS12020051) for their financial supports to Nantong University and the China Postdoctoral Science Foundation (2021T140346) and the Open Project Program of Fujian Key Laboratory of Novel Functional Textile Fibers and Materials, Minjiang University, China (FKLTFM 1917), for its financial support to GP.

REFERENCES

Amani, A., Kabiri, T., Shafiee, S., and Hamidi, A. (2019). Preparation and Characterization of PLA-PEG-PLA/PEI/DNA Nanoparticles for Improvement of Transfection Efficiency and Controlled Release of DNA in Gene Delivery Systems. *Iran J. Pharm. Res.* 18, 125–141. doi:10.22037/ijpr.2019.2365

Arias, V., Odelius, K., Höglund, A., and Albertsson, A.-C. (2015). Homocomposites of Polylactide (PLA) with Induced Interfacial Stereocomplex Crystallites. *ACS Sustain. Chem. Eng.* 3, 2220–2231. doi:10.1021/acssuschemeng.5b00498

Baimark, Y., Pasee, S., Rungseesantivanon, W., and Prakymoramas, N. (2019). Flexible and High Heat-Resistant Stereocomplex PLLA-PEG-PLLA/PDLA Blends Prepared by Melt Process: Effect of Chain Extension. *J. Polym. Res.* 26, 218. doi:10.1007/s10965-019-1881-7

Boonluksiri, Y., Prapagdee, B., and Sombatsompop, N. (2020). Effect of poly(D-lactic Acid) and Cooling Temperature on Heat Resistance and Antibacterial Performance of Stereocomplex poly(L-lactic Acid). *J. Appl. Polym. Sci.* 137, 48970. doi:10.1002/app.48970

Brzeziński, M., and Biela, T. (2015). Micro- and Nanostructures of Polylactide Stereocomplexes and Their Biomedical Applications. *Polym. Int.* 64, 1667–1675. doi:10.1002/pi.4961

Caixia Zhao, C. X., Yuan, J., Jingfeng, H., Zou, G., and Li, J. (2019). Non-isothermal and Isothermal Crystallization Behavior of Polylactic/poly(d-Lactic) Blends with Various Molecular Weights of Poly(d-Lactic) Acid. *Polym. Sci. Ser. A.* 61, 875–889. doi:10.1134/S0965545X19060178

Cao, X., Wang, W., Hu, J., Wan, J., and Cui, L. (2020). Effect of Mixed Solvents on the Structure and Properties of PLLA/PDLA Electrospun Fibers. *Fibers Polym.* 21, 970–977. doi:10.1007/s12221-020-9389-7

Chaudhary, R. G., Ali, P., Gandhare, N. V., Tanna, J. A., and Juneja, H. D. (2019). Thermal Decomposition Kinetics of Some Transition Metal Coordination Polymers of Fumaroyl Bis (Paramethoxyphenylcarbamide) Using DTG/DTA Techniques. *Arabian J. Chem.* 12, 1070–1082. doi:10.1016/j.arabjc.2016.03.008

Furuhashi, Y., Kimura, Y., Yoshie, N., and Yamane, H. (2006). Higher-order Structures and Mechanical Properties of Stereocomplex-type Poly(lactic Acid) Melt Spun Fibers. *Polymer* 47, 5965–5972. doi:10.1016/j.polymer.2006.06.001

Hamad, K., Kaseem, M., Ayyoob, M., Joo, J., and Deri, F. (2018). Polylactic Acid Blends: The Future of green, Light and Tough. *Prog. Polym. Sci.* 85, 83–127. doi:10.1016/j.progpolymsci.2018.07.001

Jing, J., Liang, S., Yan, Y., Tian, X., and Li, X. (2019). Fabrication of Hybrid Hydrogels from Silk Fibroin and Tannic Acid with Enhanced Gelation and Antibacterial Activities. *ACS Biomater. Sci. Eng.* 5, 4601–4611. doi:10.1021/acsbiomaterials.9b00604

Kang, Y., Wang, C., Qiao, Y., Gu, J., Zhang, H., Peijs, T., et al. (2019). Tissue-engineered Trachea Consisting of Electrospun Patterned Sc-Pla/go-G-IL Fibrous Membranes with Antibacterial Property and 3D-Printed Skeletons with Elasticity. *Biomacromolecules* 20, 1765–1776. doi:10.1021/acs.biomac.9b00160

Li, Z., Jiao, D., Zhang, W., Ren, K., Qiu, L., Tian, C., et al. (2021). Antibacterial and Antihyperplasia Polylactic Acid/silver Nanoparticles Nanofiber Membrane-Coated Airway Stent for Tracheal Stenosis. *Colloids Surf. B: Biointerfaces* 206, 111949. doi:10.1016/j.colsurfb.2021.111949

Liu, B., Jiang, L., and Zhang, J. (2011). Study of Effects of Processing Aids on Properties of Poly(lactic Acid)/soy Protein Blends. *J. Polym. Environ.* 19, 239–247. doi:10.1007/s10924-010-0274-0

Liu, S., Qin, S., He, M., Zhou, D., Qin, Q., and Wang, H. (2020). Current Applications of Poly(lactic Acid) Composites in Tissue Engineering and Drug Delivery. *Composites B: Eng.* 199, 108238. doi:10.1016/j.compositesb.2020.108238

Lv, S., Zhao, X., Shi, L., Zhang, G., Wang, S., Kang, W., et al. (2018). Preparation and Properties of Sc-PLA/PMMA Transparent Nanofiber Air Filter. *Polymers* 10, 996. doi:10.3390/polym10090996

Ma, Z.-Z., and Tang, R.-C. (2017). Preparation of Silver Nanoparticles by Using the Hydrolyzates of Poly(lactic Acid) and Their Application for the Antibacterial Functionalization of Poly(lactic Acid) Non-woven Fabric. *Mater. Res. Express* 4, 035009. doi:10.1088/2053-1591/aa5dd0

Maleki, H., and Barani, H. (2020). Stereocomplex Electrospun Fibers from High Molecular Weight of poly(L-Lactic Acid) and poly(D-Lactic Acid). *J. Polym. Eng.* 40, 136–142. doi:10.1515/polyeng-2019-0026

Maleki, H., Gharehaghaji, A. A., Criscenti, G., Moroni, L., and Dijkstra, P. J. (2015). The Influence of Process Parameters on the Properties of Electrospun PLLA Yarns Studied by the Response Surface Methodology. *J. Appl. Polym. Sci.* 132, a–n. doi:10.1002/app.41388

Maleki, H., Gharehaghaji, A. A., and Dijkstra, P. J. (2017). Electrospinning of Continuous Poly (L-Lactide) Yarns: Effect of Twist on the Morphology, thermal Properties and Mechanical Behavior. *J. Mech. Behav. Biomed. Mater.* 71, 231–237. doi:10.1016/j.jmbbm.2017.03.031

Mishra, R. K., Mishra, P., Verma, K., Mondal, A., Chaudhary, R. G., Abolhasani, M. M., et al. (2019). Electrospinning Production of Nanofibrous Membranes. *Environ. Chem. Lett.* 17, 767–800. doi:10.1007/s10311-018-00838-w

Monticelli, O., Putti, M., Gardella, L., Cavallo, D., Basso, A., Prato, M., et al. (2014). New Stereocomplex PLA-Based Fibers: Effect of POSS on Polymer Functionalization and Properties. *Macromolecules* 47, 4718–4727. doi:10.1021/ma500528a

Narita, J., Katagiri, M., and Tsuji, H. (2013). Highly Enhanced Accelerating Effect of Melt-Recrystallized Stereocomplex Crystallites on Poly(L-Lactic Acid) Crystallization, 2-Effects of Poly(D-Lactic Acid) Concentration. *Macromol. Mater. Eng.* 298, 270–282. doi:10.1002/mame.201200060

Pan, G., Xu, H., Ma, B., Wizi, J., and Yang, Y. (2018). Polylactide Fibers with Enhanced Hydrolytic and thermal Stability via Complete Stereo-Complexation of Poly(l-Lactide) with High Molecular Weight of 600000 and Lower-Molecular-Weight Poly(d-Lactide). *J. Mater. Sci.* 53 (7), 5490–5500. doi:10.1007/s10853-017-1944-2

Pan, G., Xu, H., Mu, B., Ma, B., Yang, J., and Yang, Y. (2017). Complete Stereo-Complexation of Enantiomeric Polylactides for Scalable Continuous Production. *Chem. Eng. J.* 328, 759–767. doi:10.1016/j.cej.2017.07.068

Phattarateera, S., and Pattamaprom, C. (2020). The Effect of Different Acrylic-Based Rubbers on the Crystallization Behavior of PLA/PDLA Stereocomplex. *J. Polym. Environ.* 28, 1592–1600. doi:10.1007/s10924-020-01707-w

Potbhare, A. K., Chaudhary, R. G., Chouke, P. B., Yerpude, S., Mondal, A., Sonkusare, V. N., et al. (2019). Phytosynthesis of Nearly Monodisperse CuO Nanospheres Using Phyllanthus Reticulatus/Conyza Bonariensis and its Antioxidant/antibacterial Assays. *Mater. Sci. Eng. C* 99, 783–793. doi:10.1016/j.msec.2019.02.010

Potbhare, A. K., Chouke, P. B., Mondal, A., Thakare, R. U., Mondal, S., Chaudhary, R. G., et al. (2020b). Rhizoctonia solani Assisted Biosynthesis of Silver Nanoparticles for Antibacterial Assay. *Mater. Today Proc.* 29, 939–945. doi:10.1016/j.matpr.2020.05.419

Potbhare, A. K., Umekar, M. S., Chouke, P. B., Bagade, M. B., Tarik Aziz, S. K., Abdala, A. A., et al. (2020a). Bioinspired Graphene-Based Silver Nanoparticles: Fabrication, Characterization and Antibacterial Activity. *Mater. Today Proc.* 29, 720–725. doi:10.1016/j.matpr.2020.04.212

Saeidlou, S., Huneault, M. A., Li, H., Sammut, P., and Park, C. B. (2012). Evidence of a Dual Network/spherulitic Crystalline Morphology in PLA Stereocomplexes. *Polymer* 53, 5816–5824. doi:10.1016/j.polymer.2012.10.030

Sanusi, O. M., Benelfellah, A., Bikiaris, D. N., and Hocine, N. A. (2020). Effect of Rigid Nanoparticles and Preparation Techniques on the Performances of Poly(lactic Acid) Nanocomposites: A Review. *Polym. Adv. Technol.* 32, 444–460. doi:10.1002/pat.5104

Saravanakumar, K., Sriram, B., Sathiyaseelan, A., Mariadoss, A. V. A., Hu, X., Han, K.-S., et al. (2021). Synthesis, Characterization, and Cytotoxicity of Starch-Encapsulated Biogenic Silver Nanoparticle and its Improved Anti-bacterial Activity. *Int. J. Biol. Macromolecules* 182, 1409–1418. doi:10.1016/j.ijbiomac.2021.05.036

Satoungar, M. T., Fattahi, S., Azizi, H., and Khajeh Mehrizi, M. (2016). Electrospinning of Polylactic Acid/silver Nanowire Biocomposites: Antibacterial and Electrical Resistivity Studies. *Polym. Compos.* 39 (S1), E65–E72. doi:10.1002/pc.24241

Sawai, D., Tamada, M., and Kanamoto, T. (2007). Development of Oriented Morphology and Mechanical Properties upon Drawing of Stereo-Complex of poly(L-Lactic Acid) and poly(D-Lactic Acid) by Solid-State Coextrusion. *Polym. J.* 39, 953–960. doi:10.1295/polymj.PJ2007038

Septiyanti, M., Septevani, A. A., Ghozali, M., Fahmiati, S., Triwulandari, E., Restu, W. K., et al. (2020). Effect of Solvent Combination on Electrospun Stereocomplex Polylactic Acid Nanofiber Properties. *Macromol. Symp.* 391, 1900134. Si. doi:10.1002/masy.201900134

Spinella, S., Lo Re, G., Liu, B., Dorgan, J., Habibi, Y., Leclère, P., et al. (2015). Polylactide/cellulose Nanocrystal Nanocomposites: Efficient Routes for Nanofiber Modification and Effects of Nanofiber Chemistry on PLA Reinforcement. *Polymer* 65, 9–17. doi:10.1016/j.polymer.2015.02.048

Srisuwan, Y., and Baimark, Y. (2018). Controlling Stereocomplexation, Heat Resistance and Mechanical Properties of Stereocomplex Polylactide Films by Using Mixtures of Low and High Molecular Weight poly(D-Lactide)s. *E-POLYMERS.* 18, 485–490. doi:10.1515/epoly-2018-0115

Su, X., Feng, L., and Yu, D. (2020). Formation of Stereocomplex crystal and its Effect on the Morphology and Property of PDLA/PLLA Blends. *Polymers* 12, 2515. doi:10.3390/polym12112515

Tsuji, H., Wada, T., Sakamoto, Y., and Sugiura, Y. (2010). Stereocomplex Crystallization and Spherulite Growth Behavior of poly(L-Lactide)-B-poly(D-Lactide) Stereodiblock Copolymers. *Polymer* 51, 4937–4947. doi:10.1016/j.polymer.2010.08.010

Xu, G., Chen, X., Zhu, Z., Wu, P., Wang, H., Chen, X., et al. (2019). Pulse Gas-Assisted Multi-Needle Electrospinning of Nanofibers. *Adv. Compos. Hybrid Mater.* 3, 98–113. doi:10.1007/s42114-019-00129-0

Yamamoto, M., Nishikawa, G., Afifi, A. M., Lee, J.-C., and Yamane, H. (2015). Effect of the Take-Up Velocity on the Higher-Order Structure of the Melt-Electrospun PLLA/PDLA Blend Fibers. *Sen-i. Gakkaishi.* 71, 127–133. doi:10.2115/fiber.71.127

Yang, Y., Zhang, M., Ju, Z., Tam, P. Y., Hua, T., Younas, M. W., et al. (2020). Poly(lactic Acid) Fibers, Yarns and Fabrics: Manufacturing, Properties and Applications. *Textile Res. J.* 91, 1641–1669. doi:10.1177/0040517520984101

Zhang, P., Tian, R., Lv, R., Na, B., and Liu, Q. (2015). Water-permeable Polylactide Blend Membranes for Hydrophilicity-Based Separation. *Chem. Eng. J.* 269, 180–185. doi:10.1016/j.cej.2015.01.111

Conflict of Interest: The authors declare that the research was conducted in the absence of any commercial or financial relationships that could be construed as a potential conflict of interest.

Publisher's Note: All claims expressed in this article are solely those of the authors and do not necessarily represent those of their affiliated organizations, or those of the publisher, the editors, and the reviewers. Any product that may be evaluated in this article, or claim that may be made by its manufacturer, is not guaranteed or endorsed by the publisher.